A new and more accurate technique to characterize airway nitric oxide using different breath-hold times

Hye-Won Shin, Peter Condorelli and Steven C. George

Journal of Applied Physiology 98:1869-1877, 2005. First published Dec 23, 2004;
doi:10.1152/japplphysiol.01002.2004

Journal of Applied Physiology publishes original papers that deal with diverse areas of research in applied physiology, especially those papers emphasizing adaptive and integrative mechanisms. It is published 12 times a year (monthly) by the American Physiological Society, 9650 Rockville Pike, Bethesda MD 20814-3991. ISSN: 8750-7587, ESSN: 1522-1601. Visit our website at http://www.the-aps.org/.

J Appl Physiol 98: 1869–1877, 2005.
First published December 23, 2004; doi:10.1152/japplphysiol.01002.2004.

A new and more accurate technique to characterize airway nitric oxide using different breath-hold times

Hye-Won Shin,[1] Peter Condorelli,[1] and Steven C. George[1,2]

Departments of [1]Biomedical Engineering and [2]Chemical Engineering and Materials Science, University of California, Irvine, California

Submitted 13 September 2004; accepted in final form 20 December 2004

Shin, Hye-Won, Peter Condorelli, and Steven C. George. A new and more accurate technique to characterize airway nitric oxide using different breath-hold times. *J Appl Physiol* 98: 1869–1877, 2005. First published December 23, 2004; doi:10.1152/japplphysiol.01002.2004.—Exhaled nitric oxide (NO) arises from both airway and alveolar regions of the lungs, which provides an opportunity to characterize region-specific inflammation. Current methodologies rely on vital capacity breathing maneuvers and controlled exhalation flow rates, which can be difficult to perform, especially for young children and individuals with compromised lung function. In addition, recent theoretical and experimental studies demonstrate that gas-phase axial diffusion of NO has a significant impact on the exhaled NO signal. We have developed a new technique to characterize airway NO, which requires a series of progressively increasing breath-hold times followed by exhalation of only the airway compartment. Using our new technique, we determined values (means ± SE) in healthy adults (20–38 yr, $n = 8$) for the airway diffusing capacity [4.5 ± 1.6 pl·s^{-1}·parts per billion (ppb)$^{-1}$], the airway wall concentration (1,340 ± 213 ppb), and the maximum airway wall flux (4,350 ± 811 pl/s). The new technique is simple to perform, and application of this data to simpler models with cylindrical airways and no axial diffusion yields parameters consistent with previous methods. Inclusion of axial diffusion as well as an anatomically correct trumpet-shaped airway geometry results in significant loss of NO from the airways to the alveolar region, profoundly impacting airway NO characterization. In particular, the airway wall concentration is more than an order of magnitude larger than previous estimates in healthy adults and may approach concentrations (~5 nM) that can influence physiological processes such as smooth muscle tone in disease states such as asthma.

gas exchange; axial diffusion; model

NITRIC OXIDE (NO) CAN BE DETECTED in the exhaled breath and is a potential noninvasive index of lung inflammation (2). However, NO exchange dynamics in the lungs are not yet fully developed, due primarily to the unique gas exchange characteristics of NO that include both airway and alveolar contributions (9, 15, 22, 23).

Current methodologies for partitioning exhaled NO into airway and alveolar contributions rely on vital capacity breathing maneuvers, which utilize a controlled exhalation flow rate (7), or a tidal breathing pattern (5). The techniques characterize the alveolar region with an alveolar concentration (C_{ANO}) and the airway region with two parameters, the airway diffusing capacity (Daw_{NO}) and either the airway wall concentration (Caw_{NO}) or the maximum airway wall flux ($J'aw_{NO}$; equal to the product Daw_{NO}·Caw_{NO}). The techniques have been used successfully to characterize NO gas exchange dynamics for healthy subjects, as well as a wide range of lung diseases (8, 10–12, 14, 19–22).

Important limitations remain in the characterization of NO exchange for both the experimental breathing maneuvers and the theoretical models. For example, Daw_{NO} can only be measured if a very low exhalation flow rate (<50 ml/s) is sampled. This requires long (>20 s) and controlled (i.e., constant flow) exhalation phases, which can be difficult to perform for young children and subjects with compromised lung function. Importantly, Daw_{NO} may potentially provide unique structural information about the airways in lung diseases such as asthma (19, 22). In addition, the most widely used analytical methods invoke a two-compartment model, which assumes a simple cylinder geometry to represent the airway anatomy, and neglects gas-phase axial diffusion of NO. Although these assumptions preserve mathematical simplicity, they likely generate significant errors in characterizing NO exchange (17, 18, 26).

Therefore, the purpose of this study is *1*) to develop a new technique that is simple to perform and focuses on determining airway NO parameters (Caw_{NO}, Daw_{NO}, and $J'aw_{NO}$), and *2*) to define important sources of errors, such as axial diffusion and the branching structure of the airway tree, that exist in some of the currently used methods to characterize NO exchange in the lung. To achieve these aims, our new technique utilizes a series of different breath-hold times (5–30 s) and analyzes only the expired air from the airways, thus shortening and simplifying the analysis of the exhalation phase. When axial diffusion is neglected, and a cylindrical airway geometry is used, the airway NO parameters determined from the new technique are consistent with those determined from a previously described single-breath technique (24). However, when axial diffusion and a trumpet-shaped geometry are considered, airway NO parameters are significantly different. In particular, Caw_{NO} is increased by more than 14-fold to compensate for losses of NO from the airways to the alveolar region due to axial diffusion. This finding has important implications pertaining to physiological processes in disease states such as smooth muscle tone in asthma.

Glossary

$A_{I,II}$	Area under the curve in phases I and II of the exhaled NO profile [parts per billion (ppb)/ml]
$A_c(z)$	Cross-sectional area of airway space (cm^2)

Address for reprint requests and other correspondence: S. C. George, Dept. of Biomedical Engineering, Univ. of California, Irvine, 204 Rockwell Engineering Center, Irvine, California 92697–2715 (E-mail: scgeorge@uci.edu).

The costs of publication of this article were defrayed in part by the payment of page charges. The article must therefore be hereby marked "*advertisement*" in accordance with 18 U.S.C. Section 1734 solely to indicate this fact.

C_{ANO}	Mixed or average fractional concentration of NO in the gas phase of the alveolar region (ppb). A steady-state concentration is achieved for breath-hold or exhalation times >10 s.
Caw_{NO}	Airway wall concentration of NO (ppb)
C_{ENO}	Exhaled NO concentration at the mouth (ppb)
$C_{in_{NO}}$	Exhaled NO concentration (ppb) which enters the analytical instrument
C_{NO}	Exhaled NO concentration (ppb) in the gas phase of the airways
$C_{obs_{NO}}$	Exhaled NO concentration (ppb) observed from the analytical instrument
$C_{s_{NO}}$	Exhaled NO concentration (ppb) which enters the sampling line leading to the analytical instrument
$C_{peak_{NO}}$	The maximum or peak exhaled NO concentration (ppb) observed by the analytical instrument
Daw_{NO}	Diffusing capacity (ml/s) of NO in the entire airway tree, which is expressed as the volume of NO per second per fractional concentration of NO in the gas phase [ml $NO \cdot s^{-1} \cdot (ml\ NO/ml\ gas)^{-1}$] and is equivalent to $pl \cdot s^{-1} \cdot ppb^{-1}$
$D_{NO,air}$	Molecular diffusivity (diffusion coefficient) of NO in air (cm^2/s)
$J'aw_{NO}$	Maximum total volumetric flux ($ppb \cdot ml \cdot s^{-1}$ or pl/s) of NO from the airways
J_{axial}	The rate of axial diffusion of NO (pl/s) across the boundary of the airway compartment and alveolar compartment defined by Fick's first law of diffusion
RMS	Root mean square error between experimental data and model prediction
$V_{I,II}$	Exhaled volume in phases I and II of the exhalation profile (ml)
V_{aw}	Volume (ml) of the airway tree defined by the cumulative volume of airway *generations 0–17* based on Weibel (27) or the subjects ideal body weight (lbs.) plus age in years (24)
z	Axial position in the lungs (cm)

METHODS

Experiment

Subjects. Eight healthy adults (age 20–38 yr, two women) participated in the study (Table 1). All subjects had a ratio of forced expiratory volume in 1 s to forced vital capacity of >0.75 at the time of testing. In addition, all subjects had no history of smoking at any time, and no history of cardiovascular, pulmonary, or neurological diseases. The Institutional Review Board at the University of California, Irvine, approved the protocol, and written, informed consent was obtained from all subjects.

Protocol. Each subject performed a series of breath-hold maneuvers (5-, 10-, 15-, 20-, and 30-s breath hold), followed by an exhalation in which the flow rate was not controlled but was generally >300 ml/s to ensure evacuation of the airway space in <2 s. A positive pressure > 5 cmH_2O was maintained during the breath hold and exhalation to prevent nasal contamination (1). A schematic of the experimental apparatus has been previously presented (24). In addition, each subject performed a single-breath maneuver (a 20-s breath hold followed by a decreasing flow rate maneuver), as previously described (24), to determine airway NO parameters as a "gold standard" for comparison to our new technique. After measuring the indexes of NO exchange dynamics, general spirometry, including forced vital capacity and forced expiratory volume in 1 s, was measured in all subjects (Vmax229; Sensormedics, Yorba Linda, CA) by using the best performance (Table 1) from three consecutive maneuvers.

Airstream analysis. A chemiluminescence NO analyzer (NOA280, Sievers, Boulder, CO) was used to measure the exhaled NO concentration. The instrument was calibrated on a daily basis by using a certified NO gas [45 parts/million (ppm) NO in 100% N_2; Sievers]. The zero-point calibration was performed with an NO filter (Sievers) immediately before the collection of a profile. The flow rate and pressure signals were measured by using a pneumotachometer (RSS100, Hans Rudolph, Kansas City, MO). The pneumotachometer was calibrated daily and set to provide the flow in units of STPD.

Empirical data analysis. Experimental exhalation profiles following breath hold were characterized empirically (model independent) by the peak or maximum observed concentration in phases I and II (Fig. 1) of the exhalation profile ($C_{peak_{NO}}$); the width of phases I and II (W_{50}) defined as the exhaled volume in which the NO concentration was >50% of $C_{peak_{NO}}$; the total exhaled volume of phases I and II ($V_{I,II}$); and the total mass or volume of NO (area under the curve) in phases I and II ($A_{I,II}$). Each of these parameters are defined in Fig. 1.

Table 1. *Physical characteristics of subjects*

Subject No.	Gender	Age, yr	Height, in.	Body Weight, lb.	Ideal Body Weight, lb.	Vaw, ml	Vaw*, ml	FVC		FEV_1		FEV_1/FVC	
								liter	%pred	liter	%pred	liter	%pred
1	M	38	69	145	160	182	198	5.16	104	4.04	100	78	96
2	F	36	59	104	100	124	136	3.50	121	2.96	118	85	98
3	M	24	71	214	172	198	196	5.61	102	4.18	88	75	87
4	M	23	70	205	166	206	189	5.84	110	5.19	114	89	104
5	F	21	62	120	110	125	131	3.54	103	3.20	105	90	101
6	M	30	67	157	148	144	178	4.08	87	3.72	95	91	109
7	M	20	75	161	177	173	197	4.90	84	4.16	83	85	99
8	M	28	66	121	145	165	173	4.68	104	3.92	104	84	100
Mean		27.5	67.4	153	147	165	175	4.66	102	3.92	101	85	99

Ideal body weight is based on gender and ethnicity. M, male; F, female; Vaw, airway volume defined by the cumulative volume of *generations 0–17*; Vaw*, airway volume defined by the subject age (yr) plus ideal body weight in lbs. (24); FVC, forced vital capacity; FEV_1, forced expiratory volume in 1 s; FEV_1/FVC, ratio of FEV_1 to FVC; %pred, percent predicted.

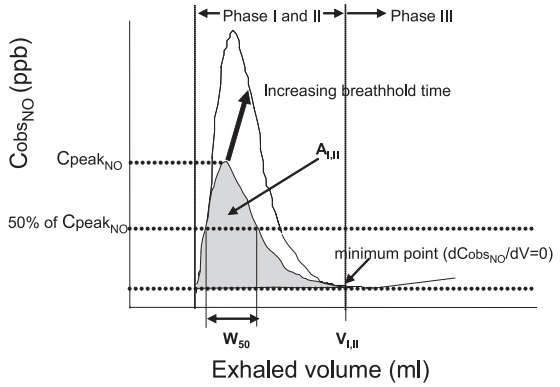

Fig. 1. Model-independent parameters characteristic of the observed exhalation profile in phases I and II are defined schematically. $C_{peak_{NO}}$, maximum concentration of nitric oxide (NO) in phases I and II; W_{50}, width of phase I and II peak calculated by taking the volume at which the exhaled concentration is larger than 50% of $C_{peak_{NO}}$; $V_{I,II}$, volume of phases I and II; $A_{I,II}$, total mass of NO (area under the curve, which is shown as a shaded region) in phases I and II; $C_{obs_{NO}}$, exhaled NO concentration observed from the analytical instrument; ppb, parts per billion. The distinction between phase I and II and phase III is the point of zero slope (minimum point) in the exhalation profile, as previously described (24). *Top* curve is a schematic representation of the exhalation profile for a larger breath-hold time.

Model Development and Simulation

Mathematical models to estimate airway NO parameters were developed for four cases: *1*) cylinder airway in the absence of axial diffusion (C); *2*) cylinder airway in the presence of axial diffusion (C-AD); *3*) trumpet airway in the absence of axial diffusion (T); and *4*) trumpet airway in the presence of axial diffusion (T-AD). The salient features of each model are presented below as well as in APPENDIX A.

Cylinder model. In this model, the airway tree is represented by a perfect cylinder (Fig. 2*A*) and is consistent with previous analytical methods to characterize NO exchange (9, 15, 22, 24). The impact of axial diffusion was quantified by comparing simulations which excluded (C) and included (C-AD) axial diffusion. The mathematical details are presented in APPENDIX A. The performance of our new technique was evaluated by comparing airway model parameters, determined using model C, to those determined using a single-breath technique (24), which also employed model C. For each subject, we characterized airway geometry by appropriately scaling the lengths and diameters of Weibel's data of the human airway tree (27), based on the conducting airway volume (V_{aw}) of *generations 0–17*, and assuming a symmetric branching pattern. The scaling procedure is based on the ratio of each subject's vital capacity to the vital capacity of the Weibel lung (3, 27) and yields values for V_{aw} that are not statistically different than estimating V_{aw} using the subject's ideal body weight (lbs.) plus age in yr (24) (Table 1). The length of the cylinder is set to the cumulative length of *generations 0–17*, which fixes the constant cross-sectional area by matching V_{aw} (Fig. 2*A*). Although CA_{NO} has been shown by many investigators to be nonzero, the values are generally <2 ppb, which are much lower than those observed in the airway tree during the breath-hold times of the current technique; thus CA_{NO} is set to zero as one of the boundary conditions. A detailed description of the mathematical model is presented in APPENDIX A.

Trumpet model. According to Weibel's data, the cross-sectional area of the airway tree increases with distance from the mouth. Thus a more anatomically realistic model of the airway tree is a "trumpet" shape (Fig. 2*B*), as described previously by several investigators (13, 16, 18). The following simple relationship between airway cross-sectional area (A_c) and axial position, z, was used to model the trumpet shape:

$$A_c = A_{c,1}\left(\frac{Z}{Z_1}\right)^{-m} \quad (1)$$

where $m = 2$ provides an excellent match (Fig. 3) to the data of Weibel (27). V_{aw} and total length (i.e., z_1) through *generation 17* was determined using the same scaling relationship described above. *Generations 17–23*, which include the respiratory and terminal bronchioles, and the alveoli are lumped together to become a single boundary, and CA_{NO} is set to zero. Additional details of the mathematical model are presented in APPENDIX A.

Parameter estimation using different breath-hold times. Utilizing five different breath-hold times, two airway NO exchange parameters (Daw_{NO} and Caw_{NO}) were determined for each subject and for each of the four models (i.e., C, C-AD, T, and T-AD) by matching the total mass of NO ($A_{I,II}$) accumulated in the airways during breath hold as a function of breath-hold time. Once Daw_{NO} and Caw_{NO} were determined, $J'aw_{NO}$ was calculated as the product $Caw_{NO}\cdot Daw_{NO}$. The model-predicted values of the area under the curve in phases I and II ($A^*_{I,II}$) are referenced to the experimental data, $A_{I,II}$, by minimizing the root mean square (RMS) error between the model prediction and experimental data defined by:

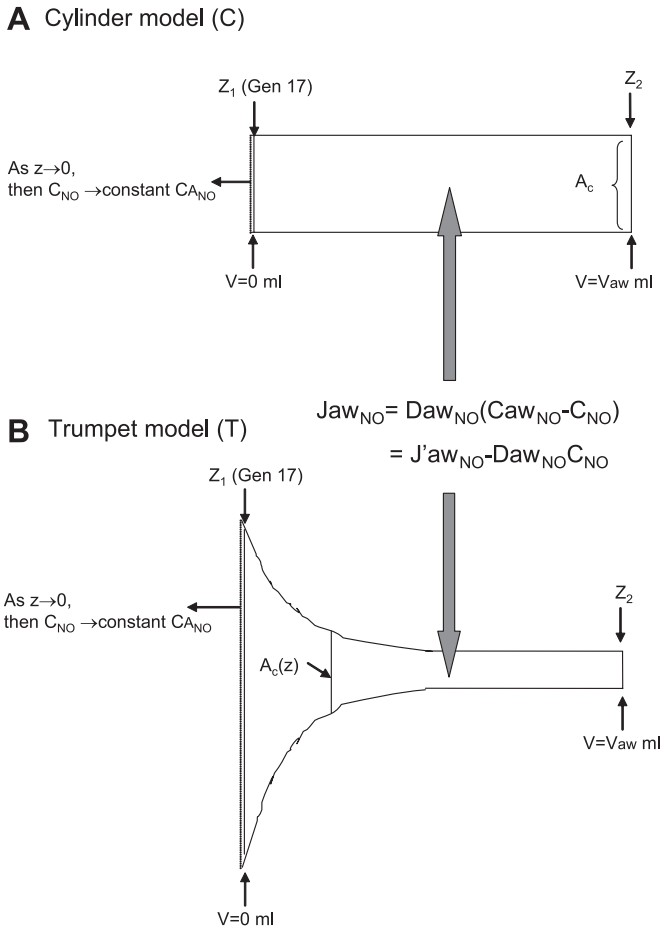

Fig. 2. Schematic of the human airway tree through 17 generations based on a cylinder model (*A*) and a trumpet model (*B*). The trumpet model is based on the symmetric bifurcating structure of Weibel (27). The cumulative cross-sectional area for any axial position, z, for the trumpet is calculated based on the cumulative cross-sectional area of all of the airways at that position. As z approaches zero, exhaled NO concentration in the gas phase of the airways (C_{NO}) approaches the constant alveolar concentration (CA_{NO}). For simplicity, CA_{NO} is set to zero for the current simulations. A_c, cross-sectional area of airway space. All other parameters are as defined in the *Glossary*.

$$\text{RMS} = \sqrt{\sum_{i=1}^{n} (A^*_{\text{I,II},n} - A_{\text{I,II},n})^2/n} \quad (2)$$

where n is the number of different breath-hold times. $A^*_{\text{I,II}}$ depends on the airway NO parameters Daw_{NO} and Caw_{NO}, as defined in APPENDIX A, and $A_{\text{I,II}}$ for each breath-hold time was the mean of the three repeated experimental maneuvers.

Statistics. Data were analyzed by using one-way and two-way repeated-measure ANOVA, followed by paired or unpaired *t*-tests, where appropriate, if the ANOVA analysis demonstrated statistical significance ($P < 0.05$). All variables were assumed to be normally distributed, and all statistical tests were performed on raw data scores. A P value < 0.05 was considered statistically significant. The intramaneuver and intrapopulation variability have been described (24) and are characterized by the 95% confidence interval expressed as a percentage of the estimated parameter value. The intramaneuver confidence interval describes the variability in a determined parameter within a single subject following the experimental protocol described above, whereas the intrapopulation confidence interval describes the anticipated range of a determined parameter within a normally distributed healthy adult population.

RESULTS

$C_{\text{peak}_{\text{NO}}}$, W_{50}, $V_{\text{I,II}}$, and $A_{\text{I,II}}$ for all eight subjects are presented in Fig. 4 to demonstrate model-independent differences in the exhaled NO profile as a function of breath-hold time. $C_{\text{peak}_{\text{NO}}}$ (Fig. 4*A*) and $A_{\text{I,II}}$ (Fig. 4*D*) were both a strong function of breath-hold time for all eight subjects. However, breath-hold time did not impact W_{50} or $V_{\text{I,II}}$ (Fig. 4, *B* and *C*).

The determined airway NO parameters for each of the four different models (C, C-AD, T, and T-AD) are presented in Fig. 5, *left*. All four models can accurately simulate the increase in $A_{\text{I,II}}$ with increasing breath-hold time. The maximum deviation between $A^*_{\text{I,II}}$ and $A_{\text{I,II}}$ for any of the breath-hold times are 10.0, 9.96, 10.0, and 6.00% for C, C-AD, T, and T-AD, respectively. Corresponding R^2 (coefficient of determination) values are 0.94, 0.95, 0.94, and 0.98 for C, C-AD, T, and T-AD, respectively. In the absence of axial diffusion, the trumpet model (T) is identical to the cylinder model (C). In the presence of axial diffusion for the cylinder geometry (C-AD), the airway NO parameters are altered by <6% (maximum deviation is a 5.8% increase for Caw_{NO}). However, the impact of axial diffusion for the trumpet geometry (T-AD) is substantial. Caw_{NO} and

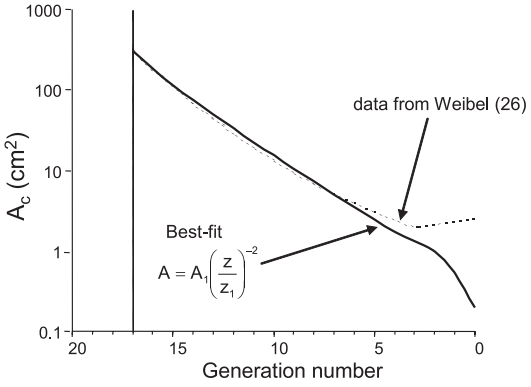

Fig. 3. A_c is shown as a function of generation number. Dotted line represents the data from Weibel (27), and the solid line represents the best fit using the power-law relation $A = A_1(z/z_1)^{-2}$, where A_1 is the cross-sectional area, and z_1 is the airway axial position at *generation 17* (volumetric position, V, equal to 0, Fig. 1).

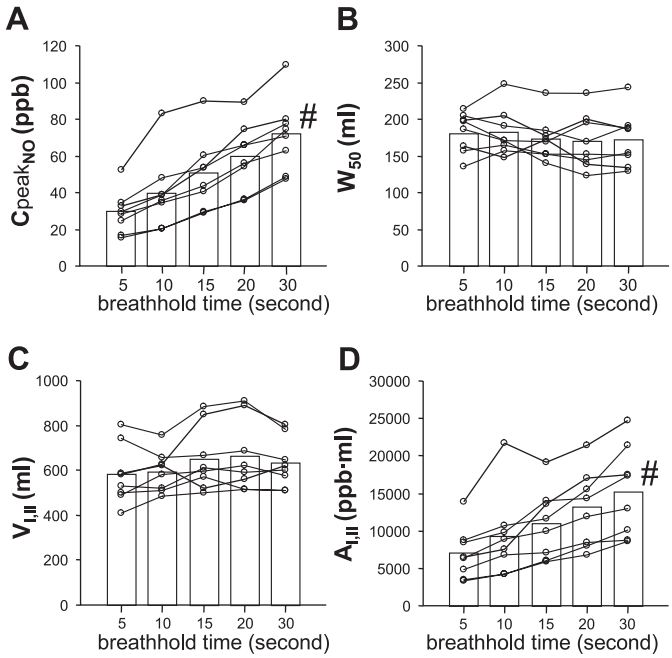

Fig. 4. Four parameters characteristic of phases I and II of the exhalation profile (Fig. 1), which are model independent, are presented for each of the different breath-hold times: $C_{\text{peak}_{\text{NO}}}$ (*A*), W_{50} (*B*), $V_{\text{I,II}}$ (*C*), and $A_{\text{I,II}}$ (*D*). The open circles and lines represent individual subjects, and the bars represent the mean. #Statistically significant changes with breath-hold time (one-way ANOVA, $P < 0.05$).

$J'\text{aw}_{\text{NO}}$ are significantly (two-way ANOVA, followed by a paired *t*-test, $P < 0.001$ for Caw_{NO} and $P = 0.01$ for $J'\text{aw}_{\text{NO}}$) increased by more than 10-fold and 2-fold, respectively; Daw_{NO} is significantly ($P = 0.01$) decreased by ~75%. For T-AD, the mean 95% intramaneuver and intrapopulation confidence intervals (20, 24) for Caw_{NO} and Daw_{NO} are 10.5 and 11.5%, and 37.5 and 83.4%, respectively.

To determine the accuracy of the breath-hold technique (independent of model), the airway NO parameters from model C were compared with those obtained from the single-breath maneuver, which also utilizes model C (Fig. 5, *right*). The determined airway NO exchange parameters were not significantly different ($P > 0.05$).

NO concentration as a function of airway volumetric position is shown in Fig. 6*A* for each of the four models when breath-hold time was set to 20 s. Recall, for all four cases, that total mass of NO within the airway tree is not different, as this is the experimental variable for which the determined model parameters are chosen to match. In the absence of axial diffusion, the trumpet model (T) and cylinder model (C) predict identical and uniform (i.e., independent of volumetric position) concentration profiles. For C-AD, the concentration of NO below *generation 5* begins to decrease due to loss of NO to the alveolar region. The presence of axial diffusion combined with the trumpet geometry further reduces the concentration of NO in the lower airway region, but this is compensated by a large increase in exhaled NO concentration in the gas phase of the airways (C_{NO}) in the upper airways (above *generation 12*). The relative magnitude of the axial flux of NO at *generation 17* (J_{axial}) utilizing a 20-s breath hold is presented in Fig. 6*B*. In the presence of axial diffusion (flux is zero in the absence of axial diffusion), the trumpet geometry increases the

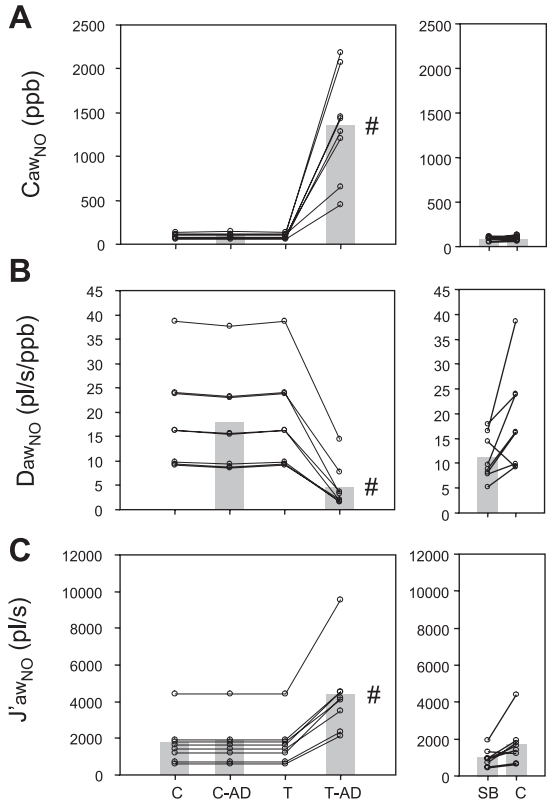

Fig. 5. *Left*: determined airway NO exchange parameters: Caw_{NO} (*A*), Daw_{NO} (*B*), and $J'aw_{NO}$ (*C*) for four different cases are shown. C, cylinder model in the absence of axial diffusion; C-AD, cylinder model in the presence of axial diffusion; T, trumpet model in the absence of axial diffusion; T-AD, trumpet model in the presence of axial diffusion. *Right*: determined airway NO exchange parameters from model C, compared with the determined values from a previously reported single-breath technique (24). The open circles and lines represent individual subjects, and the shaded bars represent the mean. #Statistical significance among models (two-way or one-way ANOVA, $P < 0.05$).

loss of NO to the alveolar region by 47-fold (J_{axial} is 2,895 vs. 62 pl/s). At very long breath-hold times, a steady state is reached, and the loss of NO to the alveolar region in the presence of the trumpet geometry is 72-fold larger than the cylinder geometry (5,364 vs. 75 pl/s).

The sampling system has previously been shown to distort the exhaled NO by introducing a lag or delay from the mouthpiece and other valving (t_{lag}), but also a significant dispersion due to the laminar flow within the sampling line that leads to the analytical instrument (5). Both of these phenomena are easily accounted for, as detailed mathematically in APPENDIX B and demonstrated in Fig. 7*A*. In this simulation, the model-determined airway NO parameters (mean for all eight subjects) for T-AD are used to simulate breath-hold times from 5 to 30 s. The NO concentration profile in the airway tree then exits the mouth (CE_{NO}) and enters the sampling system. Note the similarity in shape of this profile (Fig. 7*A*) for a 20-s breath hold to that presented in Fig. 6*A*. The sampling system then introduces a lag (t_{lag} = 1.25 s for an exhalation flow of 300 ml/s) and also significantly flattens and broadens the shape of the profile observed by the instrument [denoted $C_{obs_{NO}}(t)$ due to dispersion in the sampling line (Fig. 7*A*)]. The total mass of NO exhaled from the airway tree is not changed, but $C_{peak_{NO}}$ is reduced to 14–25% of the maximum concentration within the airway tree, depending on the breath-hold time. $C_{obs_{NO}}(t)$ predicted by the model (light shaded bars, Fig. 7*B*) agrees well with that observed experimentally (open bars).

DISCUSSION

This study presents a new method utilizing a series of different breath-hold times to characterize airway NO exchange using three parameters (Caw_{NO}, Daw_{NO}, and $J'aw_{NO}$). The parameters can be determined by matching a model to experimentally observed values of the total mass of NO exhaled from the airway following a breath hold. Four different model cases explored the impact of both axial diffusion of NO in the gas phase and airway geometry. The results demonstrate two major findings. First, the NO parameters from the new technique are not different from values of a previously described single-breath technique using a cylinder geometry in the absence of axial diffusion. Second, Caw_{NO} is more than 14-fold higher when axial diffusion and a trumpet-shaped airway geometry are considered. Thus we conclude that our new breath-hold technique has the potential to characterize airway NO exchange and that previous model simplifications regarding transport mechanisms (i.e., neglecting axial diffusion) and airway geometry (i.e., simple cylinder) have profound implications in the interpretation of airway NO exchange mechanisms. The latter emphasizes the importance of considering axial diffusion and the trumpet shape of the airway tree in models that seek to describe endogenous NO production and elimination.

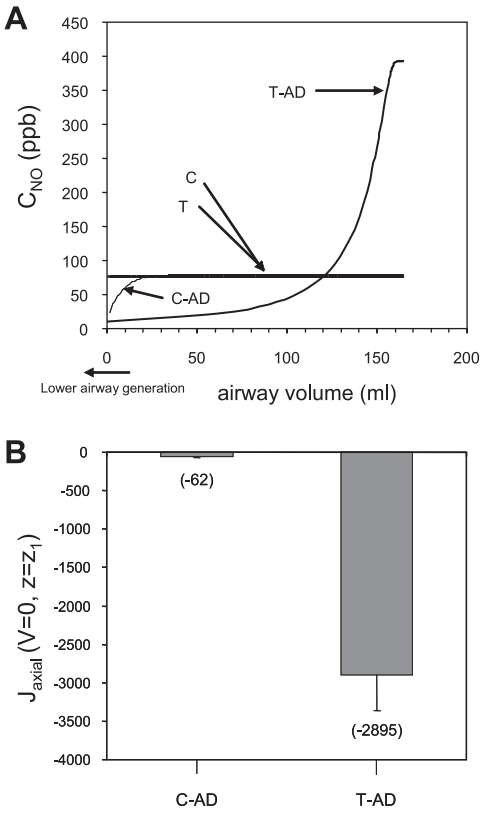

Fig. 6. *A*: C_{NO} as a function of volumetric position in the airway tree is shown for four cases: C, C-AD, T, and T-AD. *B*: axial flux of NO from diffusion (J_{axial}) at *generation 17* based on Fick's first law of diffusion is shown for both C-AD and T-AD. The significant difference is due to increased cross-sectional area at *generation 17* in the trumpet shape (Fig. 2).

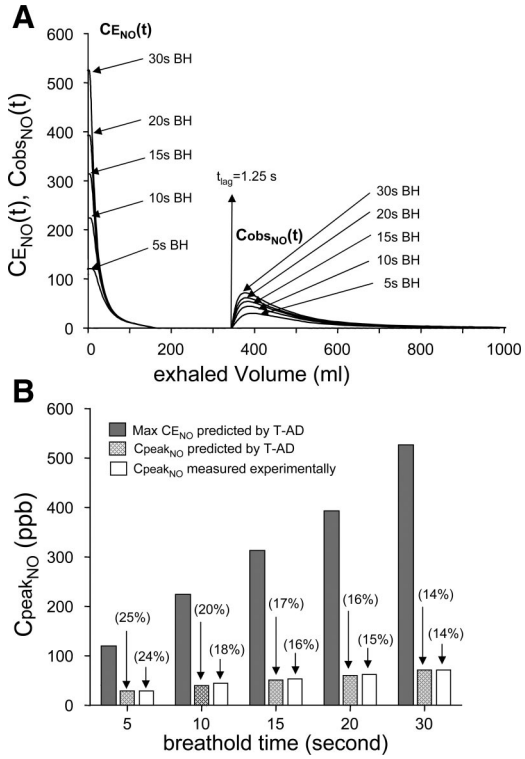

Fig. 7. *A*: using the mean value for the best-fit airway NO parameters (Daw_{NO} = 4.5 pl·s^{-1}·ppb^{-1}, Caw_{NO} = 1,340 ppb), the exhaled concentration at the mouth (CE_{NO}; before entering the sampling system) is shown for a series of breath-hold (BH) times. The shape of this profile exactly replicates the NO concentration profile with volumetric position in the airway tree at the end of the breath hold. CE_{NO} then enters the sampling system, which introduces a time lag (t_{lag} = 1.25 s) as well as a significant flattening and broadening of the peak due to dispersion within the laminar flow of the sampling line to the analytical instrument. The result is the observed concentration profile, $C_{obs_{NO}}$, by the instrument. *B*: maximum NO concentrations in the exhaled profile are shown for three cases at each of the different breath-hold times. Dark shaded bar represents the calculated maximum CE_{NO} concentration from the model simulation in *A*; light shaded bar represents the calculated maximum $C_{obs_{NO}}$ ($C_{peak_{NO}}$) from the model simulation in *A*; and the open bar represents $C_{peak_{NO}}$ from the experimental observation. $C_{peak_{NO}}$ as a fraction of the maximum CE_{NO} are shown as percentages in parentheses.

Efficacy of Breath-hold Technique

Relative to previously described single-breath techniques (9, 15, 22, 24, 25), our new breath-hold technique has two distinct advantages. First, the exhalation flow need not be controlled, providing a simpler maneuver to complete for both the subject and the investigator or clinician. Second, the technique provides improved accuracy (smaller confidence interval) for estimating Daw_{NO} relative to the single-breath technique with a 20-s breath hold and decreasing exhalation flow (24). The intramaneuver confidence interval for the single-breath technique is 168% (20, 24), compared with 11.5% for the new breath-hold technique. The improved confidence interval is due to two factors. First, the new breath-hold technique requires more individual breathing maneuvers (five breath-hold times) than the single-breath technique (one maneuver); however, each maneuver may be easier to complete for both the subject and the investigator. Second, the new technique samples a wider range of residence times (5–30 s) within the airway tree compared with the single-breath technique (20 s only). A disadvantage of the new technique is the inability to characterize the alveolar region, simply because air originating from this space is not sampled.

Finally, to preserve simplicity, the new technique considers only the total mass of NO exhaled in phases I and II and does not analyze phase III. Further refinements to the technique might include a more detailed analysis of the precise shape of the exhalation NO profile in phases I and II. For example, analysis of the width or skewness of the phase I and II peak might provide more detailed information on the location of NO production within the airway tree, which could be relevant in disease states such as asthma (19, 22). In addition, our current estimates of Daw_{NO} and Caw_{NO} are averages over the entire airway tree and do not account for dependence on transport properties of surrounding tissue (e.g., tissue thickness), which may vary with axial position.

Impact of Geometry and Diffusion on Airway NO Parameters

Axial diffusion is a fundamental mode of transport for gases in the lungs, and its relative importance depends on the competing mechanisms of transport, namely forced convection (or bulk fluid flow). The relative importance of axial diffusion increases with position into the airway tree due to the branching structure of the airway tree and thus a decreasing bulk fluid flow rate within an individual airway. Recent theoretical and experimental studies clearly demonstrate that axial diffusion has a significant impact on the exhaled NO signal and thus the characterization of NO exchange dynamics (17, 18, 26). By comparing different airway geometries in the presence and absence of axial diffusion, it is evident that axial diffusion results in a significant loss of NO to the alveolar region for the trumpet-shaped airway. This tremendous increase relative to the cylinder geometry (Fig. 6*B*) is due to the substantial increase in the cross-sectional area available for diffusion in the small airways (283 cm^2 compared with 6 cm^2 at *generation 17*). Thus, to simulate the experimentally observed total mass of NO accumulated in the airways during breath hold, the model must increase the $J'aw_{NO}$ to offset the loss to the alveolar region.

To increase the airway wall flux to compensate for losses to the alveolar region, the model can either increase the conductance (i.e., increase Daw_{NO}), increase the concentration difference between the airway wall and the gas phase in the airway lumen (i.e., increase Caw_{NO}), or some combination of both. This is described mathematically in APPENDIX A (*Eq. A1*). These options can be uniquely distinguished from each other by using the breath-hold technique. During a breath hold, NO accumulates in the gas phase, thus increasing the concentration. The final (or steady-state) concentration is determined by Caw_{NO}, and the rate at which the concentration changes is determined by Daw_{NO} (see APPENDIX A).

Figure 8 demonstrates why both Caw_{NO} and Daw_{NO} must both be changed to simulate the experimental observations. The dotted line demonstrates the best fit of the average $A_{I,II}$ as a function of breath-hold time for all eight subjects when Daw_{NO} is held constant at the best value when axial diffusion is neglected, and only Caw_{NO} is increased to increase the airway wall flux when axial diffusion is considered. Note that the mass of NO in the airway rises too quickly (too large of a conductance) to a steady-state value that is too small. Any

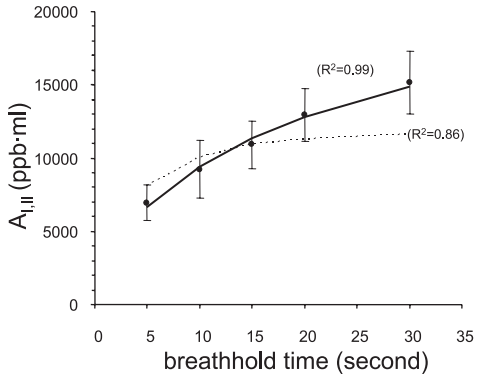

Fig. 8. Mean values of the eight healthy subjects for $A_{I,II}$ are shown as a function of breath-hold time (solid circles). The error bars represent the SD. The solid line is the best fit of these data points ($R^2 = 0.99$) using the model with a trumpet-shaped airway geometry and considering axial diffusion (T-AD) when both Daw_{NO} and Caw_{NO} are adjusted. Best-fit values for parameters Daw_{NO} and Caw_{NO} are 2.69 pl·s^{-1}·ppb^{-1} and 1,603 ppb, respectively ($J'aw_{NO} = Daw_{NO} \cdot Caw_{NO} = 4{,}312$ pl/s). The dashed line represents the best fit for the T-AD model when Daw_{NO} is held constant at the best value (18.4 pl·s^{-1}·ppb) when the cylinder-shaped airway model is used and axial diffusion is neglected, and then only Caw_{NO} is adjusted to determine the best fit. In this case, the best value for Caw_{NO} is 335 ppb, but the overall fit of the data is significantly worse ($R^2 = 0.86$), demonstrating the need to adjust both parameters to achieve the best fit of the data.

further increases in Caw_{NO} to match the experimental observations at higher breath-hold times result in a poorer match at shorter breath-hold times. Thus, to match the experimental observations, both an increase in Caw_{NO} and a decrease in Daw_{NO} (smaller conductance) are necessary.

In the presence of axial diffusion and a trumpet-shaped airway geometry, the predicted increase in the maximum airway wall flux ($J'aw_{NO} = Caw_{NO} \cdot Daw_{NO}$) is 2.6-fold (4,346 compared with 1,704 pl/s), which is consistent with previous reports that utilized models that considered axial diffusion and reported increases in $J'aw_{NO}$ that ranged from 1.5- to 5-fold (17, 18, 26). The major difference in our current simulations is the ability to more accurately separate the terms that comprise $J'aw_{NO}$ (i.e., Caw_{NO} and Daw_{NO}). The result is a mean $Caw_{NO} > 1.3$ ppm, which is more than 14-fold higher than current (mean 91 ppb) and previous estimates (range 75–225 ppb) from models that neglect axial diffusion (7).

DuBois and colleagues (6) have employed a similar experimental approach and calculated the gas-phase equilibrium NO concentrations in different regions of the airway tree, which are equivalent to Caw_{NO}. Their results are based on a model that is identical to the current model T; that is, the model is based on a trumpet-shaped geometry to determine volumetric positions and total airway volume and neglects axial diffusion. Thus the technique utilizes a simple exponential solution for the time dependence of the gas-phase concentration in the airways during a breath hold, which is equivalent to *Eq. A13* (see APPENDIX A). Based on a fit through two data points (e.g., 0- and 10-s breath hold), they report equilibrium (or Caw_{NO}) concentrations that range from 16 to 56 ppb in healthy young adults from the respiratory bronchioles to the trachea, which are consistent with our reported Caw_{NO} using model T. The reported lower concentrations in the lower airways by DuBois et al. (6) may be due to increased loss of NO to the alveolar region by axial diffusion.

This much larger wall concentration has potentially important implications for physiological processes in the airway wall, which are concentration dependent, such as the activation of soluble guanylate cyclase, which has recently been shown to be activated at concentrations as low as 3 ppm (~5 nM) (4). Thus, in asthma, where exhaled NO concentrations can be increased more than fivefold, Caw_{NO} values may reach levels that impact airway and vascular smooth muscle tone.

Gas Phase Relative to Tissue-Phase Concentration

During a breath hold, the concentration of NO in the airways increases because the concentration in the tissue phase (i.e., wall concentration, Caw_{NO}) is larger than that in the gas phase. For a very long breath-hold time, the gas-phase concentration, C_{NO}, would eventually reach Caw_{NO}. Our estimated mean Caw_{NO} is 1,340 ppb, which is much larger than the experimentally observed peak concentration of 71 ppb following the largest breath-hold time of 30 s. This discrepancy is due to two phenomena. First, the sampling system introduces significant distortion of the observed exhaled profile due to axial dispersion of the gas within the sampling line leading to the NO analyzer. This causes a pulse of NO to be significantly flattened (thus lowering the peak concentration) and broadened without altering the total mass of NO in the peak. This effect can be accurately simulated using a well-studied and validated convolution for laminar flow in a tube, as described in APPENDIX B. The result is a four- to sevenfold reduction in maximum or peak concentration. For the 30-s breath hold, the T-AD model predicts a maximum concentration of 526 ppb within the airways, but a $C_{peak_{NO}}$ (observed at the instrument) of only 72 ppb, which agrees very well with the experimentally observed value of 71 ppb.

The second reason why the observed gas concentration is less than Caw_{NO} is due to the observation that a steady state has not been reached with the gas phase. In other words, the gas phase is not at equilibrium with the tissue phase. This can be observed by simply noting that $C_{peak_{NO}}$ following a 30-s breath-hold time is significantly larger than that following the 20-s breath-hold time. The natural question then becomes: how long does it take for the gas phase to reach equilibrium with the tissue phase? This can be estimated from the T-AD model and determining the time is takes to reach 95% of the final equilibrium concentration (i.e., Caw_{NO}). This time (mean ± SD) to equilibrium is 226 ± 168 s (3.75 min) for the eight healthy subjects.

Conclusions

We have presented a new technique based on progressively increasing breath-hold times to characterize airway NO exchange. The technique is relatively simple to perform and does not require monitoring or control of exhalation flow, and determined airway NO parameters agree well with a previously described single-breath technique. In addition, the impact of two important physical and anatomical features, neglected for simplicity in previous models, have been included; namely, axial diffusion of NO in the gas phase and an increasing cross-sectional area of the airway tree with axial position (i.e., trumpet shape). In the presence of axial diffusion and a trumpet shape, the model predicts a significant back diffusion of NO

from the airways into the alveolar region, which profoundly impacts the determination of airway NO parameters. In particular, the wall concentration of NO in healthy adults is more than an order of magnitude larger than previous estimates. This concentration (>1,300 ppb) approaches that capable of activating soluble guanylate cyclase and thus smooth muscle relaxation, particularly in disease states such as asthma. We conclude that the new breath-hold technique may have potential to characterize airway NO exchange in subjects unable to perform single-breath exhalations. In addition, accurate characterization of airway NO exchange must include mathematical models, which consider axial diffusion of NO in the gas phase as well as the trumpet shape of the airway tree.

APPENDIX A: MATHEMATICAL MODEL DEVELOPMENT

Governing Equation

The unsteady-state diffusion equation during breath hold in the airway (through *generation 17*) compartment is derived by the following mass balance for NO, which includes the relationship between airway cross-sectional area and axial position (*Eq. A2*):

$$\frac{dC_{NO}}{dt} = D_{NO,air}\frac{d}{dz}\left(A_c\frac{dC_{NO}}{dz}\right) - \frac{Daw_{NO}}{V_{air}}(C_{NO} - Caw_{NO}) \quad (A1)$$

$$A_c = A_{c,1}\left(\frac{Z}{Z_1}\right)^{-m} \quad (A2)$$

where $D_{NO,air}$ is molecular diffusivity of NO in air. The *left* side of *Eq. A1* represents NO accumulation in the gas phase. The first term on the *right* side of *Eq. A1* represents axial diffusion with variable cross-sectional area, and the second term represents the radial flux of NO from the airways. Beyond *generation 17*, the airways and alveoli are lumped together to become a single boundary. For *Eq. A2*, $m = 0$ for a cylinder, and $m = 2$ for the best-fit trumpet-shaped airway (27) (Fig. 2). The initial condition for *Eq. A1* is $C_{NO}(z, t = 0) = 0$, and the boundary conditions for *Eq. A1* are as follows:

$$C_{NO}(z_1, t) = 0 \text{ (zero alveoli concentration)} \quad (A3)$$

$$\frac{dC_{NO}(z_2, t)}{dz} = 0 \text{ (no diffusional flux at end of airway)} \quad (A4)$$

For *Eq. A3*, we assume that, as z approaches zero, C_{NO} approaches the constant CA_{NO}. For simplicity, CA_{NO} is set to zero, as airway concentrations during a breath hold are much larger than reported values for the alveolar region [$C_{NO}(z_1, t) \cong C_{NO}(z = 0, t) = CA_{NO} = 0$].

Dimensionless Form of Governing Equation

The unsteady boundary value problem of *Eq. A1* is expressed in the following dimensionless form:

$$\frac{d\varphi}{d\tau} = \frac{d^2\varphi}{dx^2} - \frac{m}{x}\frac{d\varphi}{dx} - \alpha\varphi \quad (A5)$$

$$A_c = A_{c,1}x^{-m} \quad (A6)$$

where $x = \frac{z}{z_1}$, $\varphi = \frac{C_{NO} - Caw_{NO}}{-Caw_{NO}}$, $\tau = \frac{D_{NO,air}t}{Z_1^2}$, $\alpha = \frac{Daw_{NO}z_1^2}{D_{NO,air}V_{air}}$, and

$$\text{Initial condition: } \varphi(x, \tau = 0) = 0 \quad (A7)$$

$$\text{Boundary condition: } \varphi(x = 0, \tau) = 1 \quad (A8)$$

$$\frac{d\varphi(x_2, \tau)}{dx} = 0 \quad (A9)$$

Model Solution

For each of the four cases (C, C-AD, T, and T-AD), the solution of the governing equation (*Eq. A1*) has the following form

$$C_{NO} = Caw_{NO}(1 - \zeta) \quad (A10)$$

where the closed form expression for ζ depends on the model as follows.

1) Cylinder airway geometry ($m = 0$) in the absence of axial diffusion (C)

$$\zeta = e^{-\alpha\tau} \quad (A11)$$

where α depends on Daw_{NO} and is define above.

2) Cylinder airway geometry ($m = 0$) in the presence of axial diffusion (C-AD)

$$\zeta = -\frac{\sinh(\sqrt{\alpha}x_2)}{\cosh(\sqrt{\alpha}x_2)}\sinh(\sqrt{\alpha}x) + \cosh(\sqrt{\alpha}x) + \sum_{n=1}^{\infty} C_n e^{-\lambda^2\tau}x^{0.5}J_{0.5}(\gamma x) \quad (A12)$$

where, $\gamma = \sqrt{\lambda^2 - \alpha} = \sum_{n=0}^{\infty}\frac{(n + 0.5)\pi}{x_2}$, J is the Bessel function of the first kind, and

$$C_n = \frac{\int_0^{x_2}\left\{1 - \left[-\frac{\sinh(\sqrt{\alpha}x_2)}{\cosh(\sqrt{\alpha}x_2)}\sinh(\sqrt{\alpha}x) + \cosh(\sqrt{\alpha}x)\right]\right\}x^{0.5}J_{0.5}(\gamma x)dx}{\int_0^{x_2} xJ_{0.5}^2(\gamma x)dx}$$

3) Trumpet airway geometry ($m = 2$) in the absence of axial diffusion (T)

$$\zeta = e^{-\alpha\tau} \quad (A13)$$

4) Trumpet airway geometry ($m = 2$) in the presence of axial diffusion (T-AD)

$$\zeta = -\frac{\cosh(\sqrt{\alpha}x_2)}{\sinh(\sqrt{\alpha}x_2)}[\sinh(\sqrt{\alpha}x) - \sqrt{\alpha}x\cosh(\sqrt{\alpha}x)] - \sqrt{\alpha}x\sinh(\sqrt{\alpha}x) + \cosh(\sqrt{\alpha}x) + \sum_{n=1}^{\infty} C_n e^{-\lambda^2\tau}x^{1.5}J_{1.5}(\gamma x) \quad (A14)$$

where, $\gamma = \sqrt{\lambda^2 - \alpha} = \sum_{n=0}^{\infty}\frac{(n + 1)\pi}{x_2}$, and

$$C_n = \frac{\int_0^{x_2}\left(1 - \left\{-\frac{\cosh(\sqrt{\alpha}x_2)}{\sinh(\sqrt{\alpha}x_2)}[\sinh(\sqrt{\alpha}x) - \sqrt{\alpha}x\cosh(\sqrt{\alpha}x)] - \sqrt{\alpha}x\sinh(\sqrt{\alpha}x) + \cosh(\sqrt{\alpha}x)\right\}\right)x^{-0.5}J_{1.5}(\gamma x)dx}{\int_0^{x_2} xJ_{1.5}^2(\gamma x)dx}$$

APPENDIX B: DISTORTION OF EXHALED NO CONCENTRATION PROFILE BY SAMPLING SYSTEM

The experimental monitoring system, characterized in previous work (5, 24), continuously collects a small sampling flow ($\dot{V}_s$ = 4.2 ml/s) of expired air through a 1.8-mm-diameter line (volume, V_s = 5.5 ml, and space-time, $\tau_s = V_s/\dot{V}_s$ = 1.3 s). Since the sample line is maintained at laminar flow, the resulting concentration input to the NO analyzer, $C_{in_{NO}}(t)$, is delayed and distorted, and this effect can be approximated in terms of a convolution integral (5):

$$t \leq \tau_s/2: \quad C_{in_{NO}}(t) = 0 \qquad (B1)$$

$$t > \tau_s/2: \quad C_{in_{NO}}(t) = (\tau_s^2/2) \int_0^{t-\tau_s/2} \frac{C_{s_{NO}}(u)}{(t-u)^3}\, du \qquad (B2)$$

where $C_{s_{NO}}(t)$ is the NO concentration at the sampling point.

In addition, before exhaled air from the mouth (concentration, $C_{E_{NO}}$) is sampled, it traverses a dead space region (characterized by plug flow) within the mouthpiece assembly (volume, V_{ds} = 135 ml). Thus the concentration entering the sampling line, $C_{s_{NO}}$, is delayed by space-time, $\tau_{ds} = V_{ds}/\dot{V}_E$, relative to $C_{E_{NO}}$, or $C_{s_{NO}}(t) = C_{E_{NO}}(t - \tau_{ds})$. $\dot{V}_E$ represents exhalation flow rate (ml/s). Although the analyzer's response may also be characterized by a convolution integral, the instrument imparts minimal distortion on the signal; thus the instrument response is modeled as a brief additional lag of 0.15 s (5). Thus numerical integration of $C_{s_{NO}}(t) = C_{E_{NO}}(t - \tau_{ds})$ using *Eqs. B1* and *B2* yields $C_{in_{NO}}(t)$, which is translated in time to obtain the observed NO concentration from the instrument, $C_{obs_{NO}}(t)$.

GRANTS

This work was supported by National Heart, Lung, and Blood Institute Grant HL-070645. We also thank the General Clinical Research Center at the University of California, Irvine.

REFERENCES

1. **American Thoracic Society.** Recommendations for standardized procedures for the on-line and off-line measurement of exhaled lower respiratory nitric oxide and nasal nitric oxide in adults and children-1999. *Am J Respir Crit Care Med* 160: 2104–2117, 1999.
2. **Barnes PJ and Kharitonov SA.** Exhaled nitric oxide: a new lung function test. *Thorax* 51: 233–237, 1996.
3. **Bui TD, Dabdub D, and George SC.** Modeling bronchial circulation with application to soluble gas exchange: description and sensitivity analysis. *J Appl Physiol* 84: 2070–2088, 1998.
4. **Condorelli P and George SC.** In vivo control of soluble guanylate cyclase activation by nitric oxide: a kinetic analysis. *Biophys J* 80: 2110–2119, 2001.
5. **Condorelli P, Shin HW, and George SC.** Characterizing airway and alveolar nitric oxide exchange during tidal breathing using a three-compartment model. *J Appl Physiol* 96: 1832–1842, 2004.
6. **DuBois AB, Kelley PM, Douglas JS, and Mohsenin V.** Nitric oxide production and absorption in trachea, bronchi, bronchioles, and respiratory bronchioles of humans. *J Appl Physiol* 86: 159–167, 1999.
7. **George SC, Hogman M, Permutt S, and Silkoff PE.** Modeling pulmonary nitric oxide exchange. *J Appl Physiol* 96: 831–839, 2004.
8. **Girgis RE, Gugnani MK, Abrams J, and Mayes MD.** Partitioning of alveolar and conducting airway nitric oxide in scleroderma lung disease. *Am J Respir Crit Care Med* 165: 1587–1591, 2002.
9. **Hogman M, Drca N, Ehrstedt C, and Merilainen P.** Exhaled nitric oxide partitioned into alveolar, lower airways and nasal contributions. *Respir Med* 94: 985–991, 2000.
10. **Hogman M, Holmkvist T, Wegener T, Emtner M, Andersson M, Hedenstrom H, and Merilainen P.** Extended NO analysis applied to patients with COPD, allergic asthma and allergic rhinitis. *Respir Med* 96: 24–30, 2002.
11. **Lehtimaki L, Kankaanranta H, Saarelainen S, Hahtola P, Jarvenpaa R, Koivula T, Turjanmaa V, and Moilanen E.** Extended exhaled NO measurement differentiates between alveolar and bronchial inflammation. *Am J Respir Crit Care Med* 163: 1557–1561, 2001.
12. **Lehtimaki L, Turjanmaa V, Kankaanranta H, Saarelainen S, Hahtola P, and Moilanen E.** Increased bronchial nitric oxide production in patients with asthma measured with a novel method of different exhalation flow rates. *Ann Med* 32: 417–423, 2000.
13. **Paiva M and Engel LA.** Pulmonary interdependence of gas transport. *J Appl Physiol* 47: 296–305, 1979.
14. **Pedroletti C, Hogman M, Merilainen P, Nordvall LS, Hedlin G, and Alving K.** Nitric oxide airway diffusing capacity and mucosal concentration in asthmatic schoolchildren. *Pediatr Res* 54: 496–501, 2003.
15. **Pietropaoli AP, Perillo IB, Torres A, Perkins PT, Frasier LM, Utell MJ, Frampton MW, and Hyde RW.** Simultaneous measurement of nitric oxide production by conducting and alveolar airways of humans. *J Appl Physiol* 87: 1532–1542, 1999.
16. **Scherer PW, Gobran S, Aukburg SJ, Baumgardner JE, Bartkowski R, and Neufeld GR.** Numerical and experimental study of steady-state CO_2 and inert gas washout. *J Appl Physiol* 64: 1022–1029, 1988.
17. **Shin HW, Condorelli P, Rose-Gottron CM, Cooper DM, and George SC.** Probing the impact of axial diffusion on nitric oxide exchange dynamics with heliox. *J Appl Physiol* 97: 874–882, 2004.
18. **Shin HW and George SC.** Impact of axial diffusion on nitric oxide exchange in the lungs. *J Appl Physiol* 93: 2070–2080, 2002.
19. **Shin HW, Rose-Gottron CM, Cooper DM, Newcomb RL, and George SC.** Airway diffusing capacity of nitric oxide and steroid therapy in asthma. *J Appl Physiol* 96: 65–75, 2004.
20. **Shin HW, Rose-Gottron CM, Perez F, Cooper DM, Wilson AF, and George SC.** Flow-independent nitric oxide exchange parameters in healthy adults. *J Appl Physiol* 91: 2173–2181, 2001.
21. **Shin HW, Rose-Gottron CM, Sufi RS, Perez F, Cooper DM, Wilson AF, and George SC.** Flow-independent nitric oxide exchange parameters in cystic fibrosis. *Am J Respir Crit Care Med* 165: 349–357, 2002.
22. **Silkoff PE, Sylvester JT, Zamel N, and Permutt S.** Airway nitric oxide diffusion in asthma: role in pulmonary function and bronchial responsiveness. *Am J Respir Crit Care Med* 161: 1218–1228, 2000.
23. **Tsoukias NM and George SC.** A two-compartment model of pulmonary nitric oxide exchange dynamics. *J Appl Physiol* 85: 653–666, 1998.
24. **Tsoukias NM, Shin HW, Wilson AF, and George SC.** A single-breath technique with variable flow rate to characterize nitric oxide exchange dynamics in the lungs. *J Appl Physiol* 91: 477–487, 2001.
25. **Tsoukias NM, Tannous Z, Wilson AF, and George SC.** Single-exhalation profiles of NO and CO_2 in humans: effect of dynamically changing flow rate. *J Appl Physiol* 85: 642–652, 1998.
26. **Van Muylem A, Noel C, and Paiva M.** Modeling of impact of gas molecular diffusion on nitric oxide expired profile. *J Appl Physiol* 94: 119–127, 2003.
27. **Weibel ER.** *Morphometry of the Human Lung*. Berlin: Springer-Verlag, 1963.